UHASSELT
KNOWLEDGE IN ACTION

Maastricht University

Faculty of Medicine and Life Sciences
School for Life Sciences
Master of Biomedical Sciences

Master's thesis

Environmental exposures are associated with the gut microbiota of young children

Romy van Leeuwen

Thesis presented in fulfillment of the requirements for the degree of Master of Biomedical Sciences, specialization Environmental Health Sciences

SUPERVISOR :

Prof. dr. Tim NAWROT

MENTOR :

Mevrouw Thessa VAN PEE

2021
2022

Transnational University Limburg is a unique collaboration of two universities in two countries: the University of Hasselt and Maastricht University.

UHASSELT
KNOWLEDGE IN ACTION

www.uhasselt.be
Universiteit Hasselt
Campus Hasselt:
Martelarenlaan 42 | 3500 Hasselt
Campus Diepenbeek:
Agoralaan Gebouw D | 3590 Diepenbeek

Faculty of Medicine and Life Sciences
School for Life Sciences
Master of Biomedical Sciences

Master's thesis

Environmental exposures are associated with the gut microbiota of young children

Romy van Leeuwen

Thesis presented in fulfillment of the requirements for the degree of Master of Biomedical Sciences, specialization Environmental Health Sciences

SUPERVISOR :
Prof. dr. Tim NAWROT

MENTOR :
Mevrouw Thessa VAN PEE

Environmental exposures are associated with the gut microbiota of young children

Romy van Leeuwen[1], Thessa Van Pee[1], and Tim S Nawrot[1,2]

[1]Centre for Environmental Sciences, Hasselt University, Campus Diepenbeek, Agoralaan Gebouw D - B-3590 Diepenbeek, Belgium
[2]Department of Public Health and Primary Care, Leuven University, Herestraat 49-box 706, 3000, Leuven, Belgium

*Running title: *Environmental exposures and gut microbiota*

To whom correspondence should be addressed: Tim Nawrot, Tel: +3211268382; Email: tim.nawrot@uhasselt.be

Keywords: Air pollution, Black carbon, Gut microbiome

ABSTRACT

Air pollution and green space exposure might affect the indigenous gut bacteria by reducing or increasing its richness and diversity, thereby mediating the origin of diseases. However, the effects of environmental exposures on the gut microbiota in healthy children remain uninvestigated, which is the primary goal of this study. Herefore, urinary and cord blood black carbon (BC) particles were quantified via femtosecond pulsed laser illumination, while green space exposure was assessed via 'Green Map Flanders' based on the participants' residence. Meanwhile, Ion Torrent sequencing of the 16S rRNA gene determined the gut microbial composition. Spearman partial correlations and robust multivariable-adjusted linear regression models indicated that the Shannon index was negatively associated with the BC load in cord blood (-6.64%, p=0.046) and urine (-5.30%, p=0.014). The Simpson index was negatively associated with the BC load in cord blood (-1.84%, p=0.013) and urine (-1.35%, p=0.002). Furthermore, the relative abundances of *Coriobacteriaceae* (-96.24%, p=0.067) and *Christensenellaceae* (-98.01%, p=0.028) significantly changed after early-life BC exposure. The Chao index was positively associated with total green space within 50 m (47.14%, p=0.037), accompanied by positive trends between low green 50 m and Shannon diversity and total green 100 m and Chao richness. The relative abundance of the *Eubacterium coprostanoligenes group* (38999.13%, p=0.052) significantly changed after total green space exposure within 50 m. The DNeasy PowerSoil Pro kit was the most suitable for determining the skin microbiome composition. Further research is needed to confirm current findings and identify the role of microbiomes in the origination of diseases.

INTRODUCTION

Ambient air pollution consists of gasses including ozone (O_3), nitrogen dioxide (NO_2), sulfur dioxide (SO_2), and particulate matter (PM) arising from both natural and anthropogenic sources (1). PM can be subdivided into particles with an aerodynamic diameter $\leq$ 10 μm (PM_{10}), $\leq$ 2.5 μm ($PM_{2.5}$), and ultrafine particles (UFP) (1, 2). $PM_{2.5}$ includes black carbon (BC), the most harmful component of PM, which is released during the incomplete combustion of carbon-containing fossil-based fuels and biomass (3-7). After inhalation, PM_{10} mainly deposits in the upper airways, while $PM_{2.5}$ reaches the alveoli and can penetrate into the systemic circulation (1, 8). Hereby, it can exert toxic effects throughout the body via, e.g., inducing oxidative stress, leading to, for example, cardiovascular impairments, lower birth weight, and preterm birth (9, 10). Besides this, exposure to ambient air pollution is associated with a higher risk for non-communicable diseases (NCDs) like obesity, gastro-intestinal inflammatory diseases, cardiovascular diseases, and type II diabetes (11-13).

The accessibility of green spaces, like parks and forests, has been shown to reduce the amount of air pollution and noise, and it is positively associated with several health aspects (14, 15). For

example, people exposed to green spaces have a reduced risk of developing type II diabetes, depression, cardiovascular diseases, and obesity, suggesting that access to green spaces could help reduce the incidence of NDCs (13, 16, 17). Furthermore, it has cognitive and psychophysiological benefits that help to reduce stress and promotes physical activity and social cohesion (18-20). Additionally to health benefits, access to green spaces also increases work productivity leading to social benefits (21). Together these factors all lead to increased general health and wellbeing.

Despite the association between air pollution exposure or access to green spaces and various diseases, the impact on microbiota, such as the gut and skin microbiome, has hardly been researched. The gut microbiome develops during the first years of life and reaches an adult-like stage around the age of three (22). Intestinal bacteria are indispensable for several functions: assisting in the development of the innate and adaptive immune system, formation of a barrier against microbial pathogens, contribution to the intestinal epithelium integrity, biosynthesis of vitamins, and catabolism of dietary glycans (23).

Some factors that are known to influence the gut microbial composition include the mode of delivery, diet, and the use of antibiotics (24). However, the influence of environmental factors, such as air pollution and green space, on the gut microbiome has also been receiving more attention lately (11-13, 25, 26). After both short- and long-term exposure to ambient air pollution, intestinal bacterial diversity and richness were lower in animal and human studies (11, 12, 27-31). For example, a study found that prior year O_3 exposure was negatively associated with bacterial evenness and Shannon diversity in a population of overweight or obese adolescents (n=101) (12). The compositional changes make the gut microbiome less resilient because some bacterial functions might no longer be fulfilled, resulting in the origination of diseases (32). The effects of green space exposure on the gut microbiome have not been studied extensively. One study in adults (n=1177) revealed an increased gut microbiome diversity and richness in non-urbanized areas compared to urbanized areas (33).

Alike the gut microbiome, the indigenous skin bacteria protect against pathogens and help to develop the immune system (34). Factors known to influence the skin microbial composition include hygiene and UV radiation (35). Studies on the effect of ambient air pollution on the skin microbiome composition are lacking, potentially because of the low microbial mass, which can complicate research (34, 36). However, a study on healthy adults (n=40) revealed an inverse association between PM exposure during the week before sample collection and a decreased nasal microbiome diversity, which is highly related to the skin microbiome (37). Furthermore, a decreased skin bacterial diversity has already been associated with various skin diseases such as eczema, acne, and psoriasis, suggesting that skin bacteria are involved in the origin of diseases (13, 34).

On the other hand, exposure to green spaces is suggested to be associated with a higher skin microbial diversity, which might help to decrease the incidence of NCDs (13). This hypothesis can be referred to as the microbiome rewilding hypothesis (38). It has already been indicated that the skin microbiome diversity is higher amongst individuals living near forest and agricultural areas compared to those living in urban areas (39). Even exposures to green spaces of 15-30 minutes can already transfer environmental microbes onto the skin, exerting positive effects (13).

Despite all previous evidence, it remains unclear whether air pollution and green space exposure can induce changes in the gut and skin microbiota of healthy children during susceptible life periods (i.e., pregnancy and early childhood).

This study aims to determine the effects of ambient air pollution exposure and green space access on the skin and gut microbial composition in healthy four-to-six-year-olds enrolled in the ENVIR*ON*AGE (ENVIRonmental influence ON early AGEing) birth cohort. We hypothesize that higher exposure to ambient air pollution is associated with lower skin and gut microbial diversity and richness. In contrast, we expect higher exposure to green spaces to be associated with higher microbial diversity and richness in these children.

EXPERIMENTAL PROCEDURES

Study population – The study population consisted of 85 participants aged between four-to-six years enrolled in the ENVIR*ON*AGE birth cohort framework at Hasselt University. Within this

longitudinal cohort, the effects of pre and postnatal environmental exposures and lifestyle factors are investigated by following up children born in the East-Limburg Hospital (Genk, Belgium) from birth till adolescence. This study was approved by the ethical committees of East-Limburg Hospital (Genk, Belgium) and Hasselt University (Hasselt, Belgium) and was conducted according to the Declaration of Helsinki guidelines.

Immediately after birth, 42 ml of umbilical cord blood was collected in BD Vacutainer plastic whole blood tubes (BD, Franklin Lakes, NJ, USA), along with anthropometric data. In addition, the mother completed a questionnaire regarding lifestyle, health status, work, and educational level.

At the age of four-to-six years, the children were re-invited for a first follow-up, where clinical examinations took place, questionnaires were filled in, a urine sample was collected, and informed consent was given for both the follow-up as the microbiome study. Then, a skin swab sample was taken by stroking the forehead for one minute using a FLOQSwab (Copan Diagnostics, Inc., Murrieta, USA) moistened with a droplet of physiological saline. After collection, the FLOQSwab was preserved in ENat (Copan Diagnostics, Inc., Murrieta, USA) and stored at -20 °C. The participants were also handed a Faeces container (Sarstedt AG&CO, Nümbrecht, Germany) to collect a stool sample at home, which was kept in their home freezer (-20 °C) for a maximum of one week. Afterward, stool samples were collected by the researchers, transported on dry ice, and stored at -80 °C.

Air pollution exposure – To study ambient air pollution exposure during pregnancy and early childhood, BC loads in umbilical cord blood and urine samples were quantified based on white light generation of carbonaceous particles under femtosecond pulsed laser illumination.

Imaging chambers were made by applying a coverslip on a microscopic slide with double-sided tape on the outside rims, sealing it with glue, filling it with 100 µl cord blood or urine, sealing the remaining edges, and storing it at -20 °C. Two imaging chambers for cord blood and one imaging chamber for urine were made for each participant. For urine, the osmolality was determined with a K-7400S Osmometer (Knauer GHMB, Berlin, Germany).

The BC load in the imaging chambers was determined using a Zeiss LSM 510 and a Zeiss LSM 880, respectively. Both microscopes were equipped with a two-photon femtosecond pulsed laser with a central wavelength of 810 nm. The white light emitted by the BC particles was captured by using 400-410 nm and 450-650 nm band-pass emission filters. Employment of these emission filters allows collecting the second harmonic generation (SHG) from e.g. collagen type I and the two-photon excited autofluorescence (TPAF) of several cell types in urine or cord blood. Five 3x3 tile scans were in the urine imaging chambers, and three 10x10 tile scans in two different umbilical cord blood imaging chambers were collected. The BC load was determined using MatLab. Pixels above a certain threshold were detected by a peak-finding algorithm. Thresholds were set in such a way that only the 0.5% and the 45% most intense particles in TPAF and SHG were measured, respectively. Overlap of the channels indicated the generation of white light and thus the presence of BC particles. The detected BC load expressed as the number of BC particles was converted to the number of BC particles per ml.

Furthermore, residential BC exposure levels were calculated for the participant's residential address using spatiotemporal interpolation methods based on fixed air pollution monitoring station data combined with a dispersion model resulting in high-high resolution daily values of BC exposure. A more detailed description can be found in the supplementary section.

Green space access – Residential addresses of the participants were geocoded, and geographical information system (GIS) functions of ArcGIS 10.1 and python 3.4 were used for analysis. Low green (vegetation < 3 m), high green (vegetation > 3 m), and total green (sum of low and high green) were estimated in radii of (50, 100, 300, 500, 1000, 2000, and 3000 m) around the residential address were estimated based on the Green Map of Flanders 2012, consisting of raster data with a resolution of 1 m^2.

Gut microbiome – The gut microbiome richness and diversity were determined by sequencing the V3-V4 16S rRNA gene region. Briefly, automatic DNA extraction was performed with the E.Z.N.A. DNA extraction kit (Omega Bio-tek, Inc., Norcross, USA). DNA yield and purity were quantified using Nanodrop ND-1000

(ThermoFisher Scientific, Waltham, USA) to ensure a minimum DNA concentration. A standard and index polymerase chain reaction (PCR) cycle were performed to amplify the bacterial V3-V4 16S rRNA gene region. Both cycles used 10 µM goTaq Green Master Mix, 0.5 µM forward primer, 0.5 µM Reverse primer, and 1 µL template DNA as input.

First, a standard PCR was performed with the following primers: 341F (5′-TAC GGG AGG CAG CAG-3′) and 806R (5′-GGA CTA CVS GGG TAT CTA AT-3′) (Alpha DNA, Montreal, QC, Canada). During the amplicon PCR cycle, the rRNA underwent one initial denaturation (240 s at 95°C), 25 rounds of denaturation (3 s at 95°C), annealing (45 s at 53.4°C), and extension (120 s at 72°C), followed by one final extension (300 s at 72°C).

Next, an index PCR was done using a sequencing adaptor (underlined) and Ion Xpress barcoded (bold) primers (5′-CCA TCT CAT CCC TGC GTG TCT CCG ACT CAG **CTA AGG TAA CGA T**TA CGG GAG GCA GCA G-3′ and 5′-CCA CTA CGC CTC CGC TTT CCT CTC TAT GGG CAG TCG GTG ATG GAC TAC VSG GGT ATC TAA T-3′). During the index PCR cycle, the rRNA underwent one initial denaturation (240 s at 95°C), 20 rounds of denaturation (30 s at 95°C), annealing (45 s at 65°C), and extension (120 s at 72°C), followed by one final extension (300 s at 72°C). Amplicon and index amplification were achieved on a T100 Thermal Cycler (Bio-Rad).

Amplified products from each round were purified using AMPure XP beads (Beckman Coulter, Indianapolis, IN, USA). Barcoded amplicons were pooled in equimolar amounts and sequenced on an Ion 530 chip using 400 bp paired-end chemistry. Sequencing data were received as a set of Ion Torrent-sequenced FASTQ files. Sequences were demultiplexed using the Ion Torrent software and subsequently underwent quality trimming (removal of the last 15 nucleotides) and removal of primers using DADA2 1.10.1.1. Reads were de-replicated, and error rates and sequence variants were inferred using the DADA2 default parameters. Afterward, an amplicon sequence variant (ASV) table was built and taxonomy assigned using the assignTaxonomy function and the SILVA v138 training set,2, 3 and alternatively using DECIPHER4 for taxonomic classification with IDTaxa function and the SILVA_SSU_r138_2019 database. Rarefaction analysis was performed with ranacapa 0.1.0.6

Skin microbiome – We tested the QIAamp DNA Microbiome Kit and the DNeasy PowerSoil Pro Kit (both Qiagen, Hilden, Germany) to investigate which kit would give the best bacterial DNA quality and quantity. The DNA extractions were performed according to the manufacturer's instructions, except for the DNeasy PowerSoil Pro Kit: Lysis buffer CD1 was reduced to 600 µl, and phenol chloroform isoamyl alcohol replaced the remaining 200 µl. Furthermore, centrifugation times were extended to two minutes when using the MB Spin Column. Lastly, only 25 µl of solution C6 was added. The bacterial DNA extracted with both kits was sent to Qiagen (Hilden, Germany), where it was quantified and sequenced. The original protocols of both DNA extraction kits can be found in the supplementary section.

Statistical analysis – All statistical analyses were performed using R Statistical Software (version 4.0.5; R Foundation for Statistical Computing, Vienna, Austria). Descriptive statistics are reported as mean ± standard deviation (SD) for continuous variables and frequency (percentage) for categorical variables. Shannon diversity, Simpson diversity, and Chao richness were calculated using the vegan package in R. The quantified BC loads in urine were normalized based on the osmolality via the formula: BC urine – (estimate x (osmolality – mean osmolality)). To improve the normality of the distributions, we log-transformed BC loads and richness and diversity indices.

Partial Spearman correlations (r) and robust linear regressions were performed to examine the associations between the gut microbiome richness or diversity indices and the BC load in urine or cord blood after adjusting for *a priori* selected covariates: gender (boy or girl), age, maternal education (low: no high school diploma, medium: high school diploma, or high: college or university diploma), season of delivery (winter, spring, summer, or autumn), parity, ponderal index, and batch. Robust models and partial correlations were used because of the small sample size to reduce the effect of influential cases. Results are expressed as a percentual change after quadrupling of the BC loads. Afterward, a sensitivity analysis was performed for covariates that occurred less frequently in this dataset but were proven to influence the gut microbiome in other studies: ethnicity (European or non-European descent),

partus (natural or cesarean section), alcohol use during pregnancy (yes or no), use of antibiotics during pregnancy (yes or no) and use of antibiotics in the month prior to sample collection (yes or no). The same was done for the associations of the gut microbiome indices with green spaces but without adjustments for season of delivery. P-values <0.05 were statistically significant and are indicated with an asterisk.

The ANCOM-BC package was used to find differentially abundant bacterial families in participants with higher BC loads. Multiple testing correction was performed using the false discovery rate (FDR). P-values <0.05 and q-values <0.1 were statistically significant and are indicated with an asterisk.

RESULTS

Study population characteristics and exposure levels – A detailed description of the 85 participants is shown in Table 1. The participants were mostly female (52.9%) of European descents (96.5%) and born in summer or autumn (56.4%). At the time of sample collection, the children were on average 4.8 years old and had a ponderal index of 15.1 g/cm^3. On average, the participants mothers' were 30.4 years at birth, had a pre-pregnancy BMI of 23.4 kg/cm^2, and a pregnancy duration of 39.5 weeks. The participating child was generally the first born (51.8%), the majority of the mothers had a high education level (70.6%), did not use antibiotics (86.6%) or alcohol (76.2%), and did not smoke (91.8%) during pregnancy. The children were prenatally exposed to a mean BC concentration of 0.92 ppb and were exposed to 0.99 and 0.70 ppb of black carbon in the year and week before the sample collection. The average BC loads in cord blood and urine were 58040.9, and 176962 particles/ml on average.

BC as an internal biomarker for exposure – To determine whether BC is a short- or long-term biomarker for air pollution exposure, we assessed the Pearson correlation between the modeled BC exposure of the week, the month, the half-year, or the year before sample collection with the urinary BC load and the BC exposure during the whole pregnancy and per trimester with the cord blood BC load. These results show that BC in urine is significantly correlated with the exposure from last month (r=0.23; p=0.046) and last half-year (r=0.24; p=0.036), but not with last week (r=0.17; p=0.136) or last year (r=0.23; p=0.052). BC in cord blood is significantly correlated with the exposure throughout the whole pregnancy (r=0.44; p<0.001) and with all three trimesters with the strongest correlation seen with the third trimester (r=0.25; p=0.024, r=0.28; p=0.013, and r=0.39; p<0.001) (Supplementary Figure S1).

Gut bacteria – Next, we investigated which bacterial families had the highest relative abundance in the gut microbiome of the study population. Figure 1 shows that the two most common bacterial families consisted of *Lachnospiraceae* (39.07%) and *Ruminococcaceae* (24.67%), followed by *Oscillospiracea* and *Prevotellaceae*. The mean and SD for the Shannon diversity, Simpson diversity, and Chao richness indices in this population were 3.75 (0.44), 0.95 (0.03), and 181.12 (67.01).

Bacterial diversity and richness indices correlated with air pollution exposure – To determine whether air pollution exposure could affect the diversity and richness of the gut microbiome, we performed partial Spearman correlation analyses, adjusting for season of delivery, parity, ponderal index, age, gender, diploma of the mother and batch. Figure 2A shows the results from the partial correlation analysis between the diversity and richness indices and the BC loads in cord blood and urine. Bacterial diversity, as assessed by the Shannon and Simpson indices, was significantly negatively correlated with the BC contents in cord blood (r=-0.26; p= 0.028 and r=-0.29; p= 0.013, respectively) and urine (r=-0.30; p= 0.013 and r=-0.28; p= 0.019, respectively). As assessed by the Chao index, the bacterial richness was not significantly correlated with the BC load in cord blood and urine (p= 0.527 and p= 0.084, respectively).

Bacterial diversity and richness indices correlated with green space exposure – Partial Spearman correlations between low, high, or total green in buffers of 50 to 3000 m and gut microbiome diversity and richness were examined, adjusting for parity, ponderal index, age, gender, diploma of the mother, and batch. Figures 2B-H show the results of these correlations. The Shannon diversity, Simpson diversity, and Chao richness indices were not significantly correlated with low, high, or total green. Only for total green within a radius of 50 m there was a statistically significant

positive correlation with the Chao richness index (r=0.24; p=0.033).

Bacterial diversity and richness indices associated with air pollution exposure – To estimate the effect of air pollution exposure on the gut microbiome richness and diversity, robust linear regression analyzes were performed, adjusting for the same covariates. These results are shown in Table 2. The BC load in cord blood and urine were significantly negatively associated with the Shannon diversity and Simpson diversity indices. Every quadrupling in cord blood BC was associated with a -6.64% (95% CI: -12.74 to -0.12, p=0.046) change in Shannon diversity and a -1.84% (95% CI: -3.26 to -0.39, p=0.013) change in Simpson diversity. For urine these changes were -5.30% (95% CI: -9.33 to -1.09, p=0.014) and -1.35% (95% CI: -2.19 to -0.50, p=0.002), respectively. There were no significant associations between cord blood and urinary BC load (p=0.983 and p=0.234, respectively). In a sensitivity analysis, we additionally corrected for the use of alcohol or antibiotics during pregnancy or the use of antibiotics in the month preceding sample collection or we excluded participants born with a caesarian section (n=1) or participants that were not of European descents (n=3), since these covariates turned out to be relevant in other studies. Table 3 shows that these factors did not substantially impact our findings.

Bacterial diversity and richness indices associated with green space exposure – The effect of green space access on the gut microbiome richness and diversity was also estimated by performing robust linear regression analyses, adjusting for the same covariates. These results are shown in Table 4 and Supplementary Table S1 The Chao index was significantly positively associated with total green space within a radius of 50 m. Every quadrupling of total green space within 50 m resulted in a 16.51% (95% CI: 2.38 to 111.47 , p=0.037) change in Chao richness. There were no other statistically significant associations between any of the green space radii and the Chao richness. Yet, positive trends were found between low green 50 m and the Shannon diversity index (p=0.066) and between total green 100 m and the Chao richness (p=0.074).

In a sensitivity analysis, we additionally corrected for the use of alcohol or antibiotics during pregnancy or the use of antibiotics in the month preceding sample collection or we excluded participants born with a caesarian section (n=1) or participants that were not of European descents (n=3), since these covariates turned out to be relevant in other studies. Table 5 shows that these factors did not substantially impact our findings.

Gut bacterial families associated with air pollution exposure – To find out which individual bacterial families drive the associations between BC or green space exposure and the gut microbiome diversity or richness, we did a differential abundance analysis (Table 6). After quadrupling of the urinary BC load, a -96.24% change in *Coriobacteriaceae* (p=0.002) and a -98.1% change in *Christensenellaceae* (p<0.001) was seen, which remained statistically significant after FDR correction (q=0.067, and q=0.028, respectively).

A four times increase in total green space within a radius of 50 m was associated with a 38999.13% increase in *Eubacterium coprostanoligenes group* (p=0.001), which remained statistically significant after FDR correction (q=0.052).

Assessment of the most suitable DNA extraction kit for skin swab DNA extractions – To assess which DNA extraction kit, DNeasy PowerSoil Pro kit or Qiagen DNA Microbiome kit, is the most suited for the extraction of bacterial DNA, bacterial DNA extracted with both kits was sent to Qiagen for sequencing and data analysis. First, the fragment lengths and DNA quantity were analyzed after PCR. Bacterial DNA fragments extracted with the DNeasy PowerSoil Pro kit had an average fragment length of 621.2 base pairs and an average concentration of 19.2 ng/µl, whereas the extracts of the Qiagen DNA Microbiome kit had an average fragment length of 631.3 base pairs and an average concentration of 15.7 ng/µl. Furthermore, after sequencing and data analysis, the phylogenetic diversity of the extracts was compared. This diversity was not significantly different between the two kits, however, the bacterial diversity was slightly higher when using the DNeasy PowerSoil Pro kit (Figure 3). The presence of the smart control indicated that the 16S rRNA region was amplified. Because of the higher DNA concentration of the DNA fragments extracted with the DNeasy PowerSoil Pro kit and the higher phylogenetic diversity we decided to perform future extractions with the DNeasy PowerSoil Pro kit.

Table 1 –Study population characteristics (n=85)

Characteristic	Mean (SD)	No. (%)
Child		
Age (years)	4,8 (0.6)	
Female		45 (52,9)
European descent*	82 (96.5)	
Ponderal index (g/cm^3)	15.1 (1.3)	
Season of birth		
Winter	23 (27.1)	
Spring	14 (16.4)	
Summer	24 (28.2)	
Autumn	24 (28.2)	
BC exposure prenatal (ppb)	0.92 (0.25)	
BC exposure last year (ppb)	0.99 (0.16)	
BC exposure last week (ppb)	0.70 (0.18)	
BC load cord blood (particles/ml)[A]	58040.9 (25211.3)	
BC load urine (particles/ml)[A]	176962 (134125)	
Mother		
Pregnancy duration (weeks)	39.5 (1,7)	
Age at delivery (years)	30.4 (3.7)	
Pre-gestational BMI (kg/cm^2)	23.4 (3.5)	
Educational level**		
Low		2 (2.4)
Middle		23 (27.1)
High		60 (70.6)
Parity		
1		44 (51.8)
2		34 (40)
3		7 (8.2)
Breastfeeding[B]		62 (79.5)
Use of antibiotics during pregnancy[C]		11 (13.4)
Smoking behavior during pregnancy		7 (8.2)
Alcohol use during pregnancy[D]		
No alcohol		64 (76.2)
Occasionally		19 (22.6)
Not more than 1 glass/day		1 (1.2)

[A]Data only available for 79 participants, [B]Data only available for 78 participants, [C]Data only available for 82 participants, [D]Data only available for 84 participants, *The participant was considered of European descent if at least 2 of its grandparents were of European origin, **Mothers with high education levels completed college or university, middle education levels obtained a high school diploma, and low education levels did not obtain a high school diploma. BC: Black carbon

DISCUSSION

Environmental exposures were associated with the gut microbiome diversity and richness – Our study demonstrated that pre and postnatal BC exposures were negatively correlated and associated with the Simpson and Shannon diversity indices and not correlated or associated with the Chao richness index. These results could indicate an overall increase of low abundant species and an overall decrease of high abundant species without changing the total number of bacterial species present in the fecal samples (40). The results of comparable studies generally show a decrease or no significant effect on Shannon and

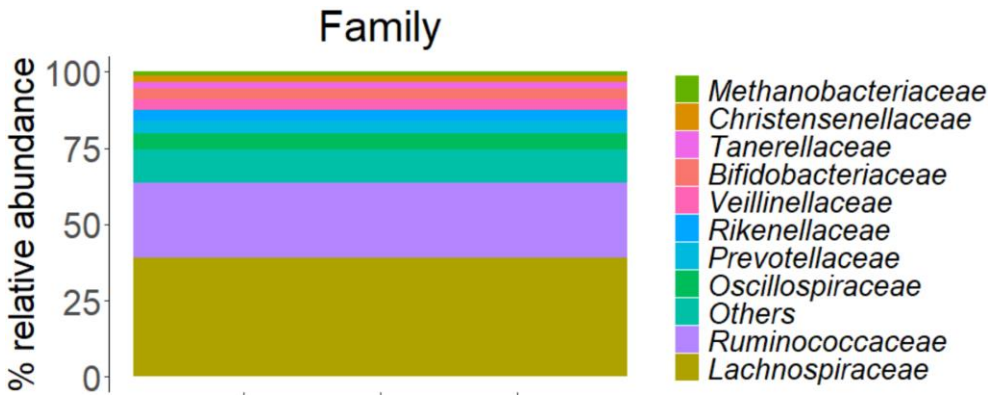

Fig. 1 – Ten most common gut microbes in the study population as determined by 16S RNA Ion Torrent sequencing expressed as percentual relative abundance.

Chao indices (12, 31, 41) and no significant effect on the Simpson index (30, 42-47). For example, in the study by Liu *et al.* (31), they investigated the effect of prior 2-year $PM_{2.5}$ and PM_1 exposure on the gut microbiome diversity and richness in healthy and diabetic adults based on a land-use regression model and found that $PM_{2.5}$ and PM_1 were negatively associated with the Chao-1 richness index and the Shannon diversity index. Furthermore, the pollutants were negatively associated with observed OTUs, another indicator of bacterial richness, and with phylogenetic diversity whole tree, another indicator of bacterial diversity (31).

We also showed that the Shannon, Simpson, and Chao indices were not correlated or associated with green space accessibility, except for a positive correlation between the Chao index and total green space within a radius of 50 m. Furthermore, a trend was seen between total green within a radius of 100 m and an increase in Chao richness index, and low green within a radius of 50 m and the Shannon diversity index. An intervention study through which children were brought in contact with nature and a study that compared the gut microbiome of people living in urbanized and non-urbanized areas also observed increases in the Chao richness index (26, 33). Another study consisting of four-month-old participants (n=355) looked at green spaces within 500 and 1000 m based on the urban Primary Land and Vegetation Inventory. They found no correlation between green space access and the Chao richness index. However, they did find a negative correlation between green spaces with the Shannon and Simpson index, which they hypothesize might occur because exposure to green spaces could lead to the overgrowth of specific microbes (25).

Environmental exposures were associated with the relative abundance of gut bacterial families – After FDR correction, postnatal BC exposure was significantly negatively associated with the relative abundance of *Coriobacteriaceae* and *Christensenellaceae*. Total green within 50 m was significantly positively associated with the relative abundance of the *Eubacterium coprostanoligenes group* after FDR correction.

In another study, prior year exposure to freeway traffic-related air pollution was correlated with increased *Coriobacteriaceae* in overweight adolescents (n=43) (11). This bacterial family has been linked with cholesterol metabolism and is important in processes such as the conversion of bile salts and steroids (11, 48, 49). Furthermore, Coriobacteriaceae were found to be associated with increased serum insulin and c-peptide levels in overweight pregnant women (n=70) (11, 50). Positive associations between air pollution exposure and Coriobacteriaceae were found in a study where mice were exposed to benzoapyrene. This positive association might be explained by the induction of cytochrome P450 to degrade benzoapyrene (51). Negative associations with *Coriobacteriaceae* have been found in hamsters fed with grain sorghum, which has cholesterol-lowering and cardioprotective properties (49, 52).

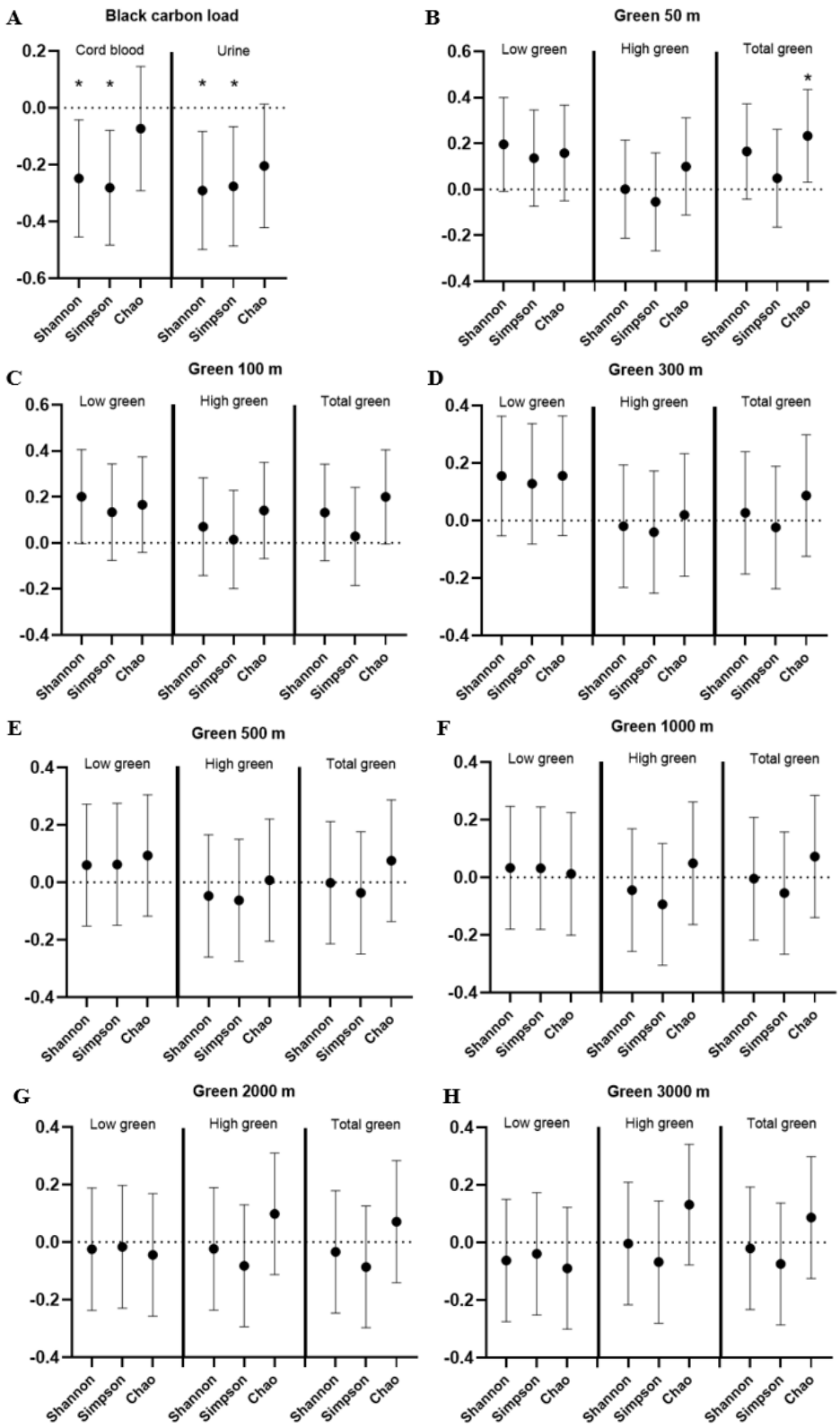

Fig. 2 – Correlation of black carbon and green spaces with the gut microbiome diversity and richness. **A)** A higher black carbon load in urine was significantly negatively associated with the Shannon and Simpson index, but not significantly correlated with the Chao index. **B-H)** Increased green space access was not correlated with the gut microbiome richness or diversity, except a significant positive correlation of green space within 50 m with the Chao index.

Table 2 – Percentual changes in diversity and richness indices after quadrupling of BC loads

	Estimate	Lower 95% CI	Upper 95% CI	p-value
Cord blood				
Shannon	-6.64	-12.74	-0.12	0.046*
Simpson	-1.84	-3.26	-0.39	0.013*
Chao	-0.22	-17.95	21.34	0.982
Urine				
Shannon	-5.30	-9.33	-1.09	0.014*
Simpson	-1.35	-2.19	-0.50	0.002*
Chao	-7.45	-18.54	5.14	0.234

Robust linear regression analyses between cord blood or urinary BC loads and Shannon diversity, Simpson diversity or Chao richness indices are shown after adjustment for season of delivery, parity, ponderal index, age, gender, diploma of the mother and batch. Results are expressed as percentual change for each quadrupling in BC load. CI: Confidence interval; BC: Black carbon
* Significant p-values ($p<0.05$).

Table 3 – Sensitivity analysis of associations between BC loads and Shannon or Simpson diversity indices

	Cord blood		Urine	
	Estimate	**p-value**	**Estimate**	**p-value**
Exclusion of participants				
Partus				
Shannon	-0.05	0.045*	-0.04	0.016*
Simpson	-0.01	0.014*	-0.01	0.002*
Ethnicity				
Shannon	-0.05	0.064	-0.04	0.010*
Simpson	-0.01	0.024*	-0.01	0.001*
Addition of covariates				
Alcohol use during pregnancy				
Shannon	-0.05	0.046*	-0.04	0.019*
Simpson	-0.01	0.014*	-0.01	0.003*
Use of antibiotics during pregnancy				
Shannon	-0.06	0.033*	-0.04557	0.006117*
Simpson	-0.01	0.013*	-0.01081	0.001722*
Use of antibiotics in the month preceding sample collection				
Shannon	-0.04	0.089	-0.03	0.029*
Simpson	-0.01	0.049*	-0.01	0.003*

Sensitivity analyses of the robust linear regression results between BC loads and Shannon or Simpson diversity indices, adjusted for partus, ethnicity, alcohol use during pregnancy, use of antibiotics during pregnancy, and use of antibiotics in the month preceding sample collection by additionally correcting for the use of alcohol or antibiotics during pregnancy, or the use of antibiotics in the month preceding sample collection, or by excluding participants born with a cesarian section or participants that are not of European descents. BC: Black carbon
* Significant p-values ($p<0.05$)

Table 4– Percentual changes in diversity and richness indices after quadrupling of green space exposure

	Estimate	Lower 95% CI	Upper 95% CI	p-value
Low green 50 m				
Shannon	16.51	-0.99	37.10	0.066+
Total green 50 m				
Chao	47.14	2.38	111.47	0.037*
Total green 100 m				
Chao	49.41	-3.78	132.01	0.074+

Robust linear regression analyses between green spaces and Shannon diversity, Simpson diversity, or Chao richness are shown after adjustment for parity, ponderal index, age, gender, diploma of the mother and batch. Results are expressed as a percentual change for each quadrupling in green space. CI: Confidence interval; BC: Black carbon

* Significant p-values ($p<0.05$)

+ p-values indicating a trend

Table 5 – Sensitivity analysis of associations between green spaces and diversity or richness indices

	Total green 50 m	
	Estimate	**p-value**
Exclusion of participants		
Partus		
Chao	0.15	0.039*
Ethnicity		
Chao	0.18	0.018*
Addition of covariates		
Alcohol use during pregnancy		
Chao	0.15	0.044*
Use of antibiotics during pregnancy		
Chao	0.14	0.104
Use of antibiotics in the month preceding sample collection		
Chao	0.16	0.058+

Sensitivity analyses of the robust linear regression results between green space and the Shannon diversity, Simpson diversity or Chao richness indices, adjusted for partus, ethnicity, alcohol use during pregnancy, use of antibiotics during pregnancy, and use of antibiotics in the month preceding sample collection by additionally correcting for the use of alcohol or antibiotics during pregnancy, or the use of antibiotics in the month preceding sample collection, or by excluding participants born with a cesarian section or participants that are not of European descents. BC: Black carbon

* Significant p-values ($p<0.05$)

Christensenellaceae is one of the most common gut bacteria and is involved in fermentation processes, such as the fermentation of sugars into short-chain fatty acids (53). The relative abundance of this bacterial is found to be decreased in individuals with a higher BMI, adiposity, waist circumference, and serum lipids and in individuals with metabolic syndrome (53-57). Because of their fermentation function, *Christensenellaceae* is responsive to diet, resulting in higher relative abundances in diets high in protein and fibers (53). However, this bacterial family has not been linked to environmental factors before.

Eubacterium coprostanoligenes group has cholesterol-reducing properties by metabolizing cholesterol into coprostanol. Coprostanol is difficult to be absorbed in the intestines and will be

Table 6 – Changes in relative abundance of gut bacterial families after environmental exposures

Exposure measurement	Family	Coefficient	p-value	q-value	% change
BC cord blood	*Coriobacteriaceae*	2.58	0.022*	0.386	3475.32
BC cord blood	*Christensenellaceae*	-2.44	0.046*	0.386	-96.60
BC cord blood	*Ethanoligenenaceae*	-1.15	0.045*	0.386	-79.69
BC cord blood	*Anaerovoracaceae*	-0.91	0.033*	0.386	-71.68
BC urine	*Methanobacteriaceae*	-1.28	0.033*	0.420	-83.07
BC urine	*Coriobacteriaceae*	-2.37	0.002*	0.067+	-96.24
BC urine	*Coriobacteriales Incertae Sedis*	-0.97	0.033*	0.420	281.88
BC urine	*Rikenellaceae*	-1.33	0.049*	0.420	-84.22
BC urine	*Christensenellaceae*	-2.83	<0.001*	0.028+	-98.01
BC urine	*Enterobacteriaceae*	1.73	0.050*	0.420	995.49
Total green 50 m	*Methanobacteriaceae*	-1.32	0.025*	0.305	-84.06
Total green 50 m	*Micrococcaceae*	-1.41	0.021*	0.305	-85.83
Total green 50 m	*Coriobacteriales Incertae Sedis*	1.83	0.031*	0.305	1168.17
Total green 50 m	*Barnesiellaceae*	3.49	0.031*	0.305	12444.83
Total green 50 m	*Prevotellaceae*	4.11	0.048*	0.328	29561.99
Total green 50 m	*[Eubacterium] coprostanoligenes group*	4.31	0.001*	0.052+	38999.13
Total green 50 m	*Anaerovoracaceae*	1.50	0.044*	0.328	700.19

Changes in the relative abundance of the gut microbial families are shown after adjustment for parity, height, weight, age, gender, diploma of the mother and batch according to Analysis of Compositions of Microbiomes with Bias Correction (ANCOM-BC). In the models for urinary and cord blood BC load, we additionally adjusted for season of delivery. Results are expressed as percentual change for each quadrupling in black carbon load. BC: Black carbon
* Significant p-values ($p<0.05$)
+ Significant p-values after FDR correction ($p<0.1$)

excreted via the feces resulting in cholesterol removal. Therefore, a higher relative abundance of the *Eubacterium coprostanoligenes* group is linked to a decreased risk of cardiovascular diseases (58). This bacterial family has, however, not been linked to environmental exposures yet.

Potential mechanisms underlying the associations between environmental exposures and the gut microbiome – Although the underlying mechanisms by which air pollution or green spaces can change the gut microbiome are not fully understood, it is known that PM can cross the respiratory membrane upon inhalation and enter the systemic circulation, where it can cause oxidative stress and inflammation. From the systemic circulation, PM can enter the enterocytes through the M cells on the Peyer's patches. In addition, PM may enter the gut via mucociliary clearance (28, 59). In the study by Wang *et al.* (59), they found that 20 µl of 1 mg/ml $PM_{2.5}$ administered via oropharynx instillation every other day, resulted in increased levels of the peroxidation products malondialdehyde, 4-Hydroxynonenal, and deoxyguanosine in C57Bl/6J mice (n=10) after four weeks of exposure. This oxidative stress can lead to the initiation of pro-inflammatory cascades, as seen in the study by Ran *et al.* (45). This study showed an increase in inflammatory cytokines, including interleukin 6, interleukin 1 beta, and tumor necrosis factor-alpha, after eight weeks of whole-body inhalation of 226.50 $\mu g/m^3$ of $PM_{2.5}$ in BALB/c mice (n=22). Intestinal permeability is also linked to oxidative stress and air pollution exposure (60). For example, PM increased intestinal permeability and colonic cell apoptosis and decreased tight junction protein 1 expression in the gut of C57Bl/6J mice (n=12) after 48 hours of incubation of 200 µg of PM administered via gavage (61). Disruption of the epithelial barrier might further lead to gut inflammation, caused by an upregulation of toll-like receptor 4, resulting in the recruitment of

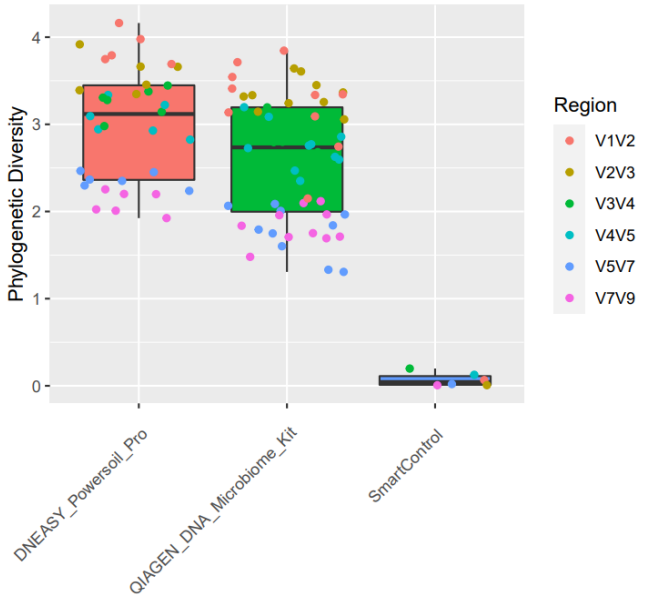

Fig. 3 – Comparison of the DNeasy PowerSoil Pro kit (n=6), and the Qiagen DNA Microbiome kit (n=10).

inflammatory cytokines (62, 63). Another potential mechanism through which air pollutants might alter the gut microbiota is the potential of BC to change the development of bacterial biofilms, which can interfere with bacterial survival (59). A decrease in perceived stress might be a potential pathway by which green space exposure can induce changes in the gut microbiome (26).

BC as internal exposure biomarker – The frequently used spatiotemporal interpolation methods based on residential addresses might lead to exposure misclassification by neglecting individual and time-activity mobility patterns (64). Therefore, we chose to use BC, the most harmful component of air pollution, as an internal exposure biomarker. By using an internal exposure biomarker, these mobility patterns are taken into consideration. Urinary BC loads were found to reflect medium- to long-term exposure since it was significantly positively correlated with BC exposure during the month and the half-year before sample collection. Furthermore, a trend was seen for BC exposures during the year before sample collection. This result is in agreement with the findings of a previous study, in which urinary black carbon also correlated positively with previous month and year BC exposure (64). The BC loads in umbilical cord blood reflected exposure throughout the complete pregnancy and could thus be considered an indicator of prenatal exposure.

Assessment of the most suitable DNA extraction kit for skin swab DNA extractions – Finally, we determined that the DNeasy PowerSoil Pro kit was the most suitable for bacterial DNA extractions, based on extract concentrations and phylogenetic diversity. Previous studies suggest an interaction between indigenous skin bacteria and air pollution. For example, He *et al.* (65) observed that the bacterial viability of bacteria comprising the normal skin microbiome significantly decreased after two hours of exposure to O_3. However, it is unknown whether ambient air pollution can lead to skin microbiome dysbiosis as suggested for the intestinal microbiome. For green space, there is one study that suggests that exposure increases the microbial richness and phylogenetic diversity (13). In this study, participants (n=3) were exposed to air, soil, and leaves from various types of green spaces.

Relevance, limitations and future directions – The preceding results are important because current changes in the composition of the gut microbiome may influence the development of diseases in later life (13). These diseases are mainly cardiovascular and metabolic disorders but also neurological disorders (11-13, 59). Even in our young study population, prenatal exposure and exposure in early life are already associated with the development of the gut microbiome. Therefore, it is essential to limit the amount of air pollution as much as

possible, for example, by tightening the current air pollution guidelines.

We acknowledge some limitations in our study, beginning with the relatively small sample size of 85 participants. Furthermore, we are aware of potential ambient BC contamination of the urine samples. Since the collection takes place in public toilets, possible contamination cannot be prevented. We did take the contamination risk into account during the processing of the samples by only processing them in a laminar flow cabinet. In addition, it would be important to study the influence of diet on the association between air pollution and the microbiome. Furthermore, it might be possible to examine whether and how changes in the microbiome could lead to adverse health effects. Lastly, potential associations between air pollution or green space exposure and the skin microbiome can be investigated.

CONCLUSION

Associations have been found between air pollution exposure and the gut microbiome, as seen in a decreased microbiome diversity and decreased relative abundances of gut bacterial families *Coriobacteriaceae* and *Christensenellaceae*. Furthermore, total green space within short proximity was associated with increased microbiome richness and an increased relative abundance of the *Eubacterium coprostanoligenes group*. Moreover, the DNeasy PowerSoil Pro kit turned out to be the most suited for bacterial DNA extractions from skin swabs. Further research will be needed to identify how green space and air pollution have an effect on the intestinal microbiome, identify the potential health effects of a changed microbiome, and find the potential associations between green space or air pollution exposure and the skin microbiome.

Acknowledgements – RvL acknowledges the Center for Environmental Sciences for the availability of the equipment, JVD for the DNA extraction and sequencing of the stool samples, and Qiagen for sequencing and data analysis of the skin swabs. RvL is also grateful for the opportunity to work in the research group of Prof. Dr. Tim Nawrot and would like to thank Thessa Van Pee for her guidance.

Author contributions – TVP and TN conceived and designed the research. RvL and TVP performed skin swab DNA extractions and data analysis. RvL wrote the paper. All authors carefully edited the manuscript.

REFERENCES

1. WHO. Ambient (outdoor) air pollution 2021 [cited 2021 Oct, 25]. Available from: https://www.who.int/news-room/fact-sheets/detail/ambient-(outdoor)-air-quality-and-health.
2. Cassee FR, Heroux ME, Gerlofs-Nijland ME, Kelly FJ. Particulate matter beyond mass: recent health evidence on the role of fractions, chemical constituents and sources of emission. Inhal Toxicol. 2013;25(14):802-12.
3. Glaser B, Dreyer A, Bock M, Fiedler S, Mehring M, Heitmann T. Source apportionment of organic pollutants of a highway-traffic-influenced urban area in Bayreuth (Germany) using biomarker and stable carbon isotope signatures. Environ Sci Technol. 2005;39(11):3911-7.
4. Long CM, Nascarella MA, Valberg PA. Carbon black vs. black carbon and other airborne materials containing elemental carbon: physical and chemical distinctions. Environ Pollut. 2013;181:271-86.
5. Medalia AI, Rivin D, Sanders DR. A comparison of carbon black with soot. Sci Total Environ. 1983;31(1):1-22.
6. Niranjan R, Thakur AK. The Toxicological Mechanisms of Environmental Soot (Black Carbon) and Carbon Black: Focus on Oxidative Stress and Inflammatory Pathways. Front Immunol. 2017;8:763.
7. Watson AY, Valberg PA. Carbon black and soot: two different substances. AIHAJ. 2001;62(2):218-28.
8. Du Y, Xu X, Chu M, Guo Y, Wang J. Air particulate matter and cardiovascular disease: the epidemiological, biomedical and clinical evidence. J Thorac Dis. 2016;8(1):E8-E19.

9. Feng S, Gao D, Liao F, Zhou F, Wang X. The health effects of ambient PM2.5 and potential mechanisms. Ecotoxicol Environ Saf. 2016;128:67-74.
10. Wang G, Zhao J, Jiang R, Song W. Rat lung response to ozone and fine particulate matter (PM2.5) exposures. Environ Toxicol. 2015;30(3):343-56.
11. Alderete TL, Jones RB, Chen Z, Kim JS, Habre R, Lurmann F, et al. Exposure to traffic-related air pollution and the composition of the gut microbiota in overweight and obese adolescents. Environ Res. 2018;161:472-8.
12. Fouladi F, Bailey MJ, Patterson WB, Sioda M, Blakley IC, Fodor AA, et al. Air pollution exposure is associated with the gut microbiome as revealed by shotgun metagenomic sequencing. Environ Int. 2020;138:105604.
13. Selway CA, Mills JG, Weinstein P, Skelly C, Yadav S, Lowe A, et al. Transfer of environmental microbes to the skin and respiratory tract of humans after urban green space exposure. Environ Int. 2020;145:106084.
14. Liu H-L, Shen Y-S. The Impact of Green Space Changes on Air Pollution and Microclimates: A Case Study of the Taipei Metropolitan Area. Sustainability. 2014;6(12):8827-55.
15. Veen EJ, Ekkel ED, Hansma MR, de Vrieze AGM. Designing Urban Green Space (UGS) to Enhance Health: A Methodology. Int J Environ Res Public Health. 2020;17(14).
16. De la Fuente F, Saldías MA, Cubillos C, Mery G, Carvajal D, Bowen M, et al. Green Space Exposure Association with Type 2 Diabetes Mellitus, Physical Activity, and Obesity: A Systematic Review. International Journal of Environmental Research and Public Health. 2021;18(1):97.
17. Zhang J, Yu Z, Zhao B, Sun R, Vejre H. Links between green space and public health: a bibliometric review of global research trends and future prospects from 1901 to 2019. Environmental Research Letters. 2020;15(6):063001.
18. Hedblom M, Gunnarsson B, Iravani B, Knez I, Schaefer M, Thorsson P, et al. Reduction of physiological stress by urban green space in a multisensory virtual experiment. Scientific Reports. 2019;9(1):10113.
19. Jennings V, Bamkole O. The Relationship between Social Cohesion and Urban Green Space: An Avenue for Health Promotion. Int J Environ Res Public Health. 2019;16(3).
20. Mytton OT, Townsend N, Rutter H, Foster C. Green space and physical activity: an observational study using Health Survey for England data. Health Place. 2012;18(5):1034-41.
21. Beyer KMM, Kaltenbach A, Szabo A, Bogar S, Nieto FJ, Malecki KM. Exposure to Neighborhood Green Space and Mental Health: Evidence from the Survey of the Health of Wisconsin. International Journal of Environmental Research and Public Health. 2014;11(3):3453-72.
22. Jandhyala SM, Talukdar R, Subramanyam C, Vuyyuru H, Sasikala M, Nageshwar Reddy D. Role of the normal gut microbiota. World J Gastroenterol. 2015;21(29):8787-803.
23. Dave M, Higgins PD, Middha S, Rioux KP. The human gut microbiome: current knowledge, challenges, and future directions. Transl Res. 2012;160(4):246-57.
24. Hasan N, Yang H. Factors affecting the composition of the gut microbiota, and its modulation. PeerJ. 2019;7:e7502.
25. Nielsen CC, Gascon M, Osornio-Vargas AR, Shier C, Guttman DS, Becker AB, et al. Natural environments in the urban context and gut microbiota in infants. Environ Int. 2020;142:105881.
26. Sobko T, Liang S, Cheng WHG, Tun HM. Impact of outdoor nature-related activities on gut microbiota, fecal serotonin, and perceived stress in preschool children: the Play&Grow randomized controlled trial. Sci Rep. 2020;10(1):21993.
27. Chen D, Xiao C, Jin H, Yang B, Niu J, Yan S, et al. Exposure to atmospheric pollutants is associated with alterations of gut microbiota in spontaneously hypertensive rats. Exp Ther Med. 2019;18(5):3484-92.
28. Fitch MN, Phillippi D, Zhang Y, Lucero J, Pandey RS, Liu J, et al. Effects of inhaled air pollution on markers of integrity, inflammation, and microbiota profiles of the intestines in Apolipoprotein E knockout mice. Environ Res. 2020;181:108913.

29. Li N, Yang Z, Liao B, Pan T, Pu J, Hao B, et al. Chronic exposure to ambient particulate matter induces gut microbial dysbiosis in a rat COPD model. Respir Res. 2020;21(1):271.
30. Liu J, Su X, Lu J, Ning J, Lin M, Zhou H. PM2.5 induces intestinal damage by affecting gut microbiota and metabolites of rats fed a high-carbohydrate diet. Environ Pollut. 2021;279:116849.
31. Liu T, Chen X, Xu Y, Wu W, Tang W, Chen Z, et al. Gut microbiota partially mediates the effects of fine particulate matter on type 2 diabetes: Evidence from a population-based epidemiological study. Environ Int. 2019;130:104882.
32. Lozupone CA, Stombaugh JI, Gordon JI, Jansson JK, Knight R. Diversity, stability and resilience of the human gut microbiota. Nature. 2012;489(7415):220-30.
33. Du Y, Ding L, Na L, Sun T, Sun X, Wang L, et al. Prevalence of Chronic Diseases and Alterations of Gut Microbiome in People of Ningxia China During Urbanization: An Epidemiological Survey. Front Cell Infect Microbiol. 2021;11:707402.
34. Byrd AL, Belkaid Y, Segre JA. The human skin microbiome. Nat Rev Microbiol. 2018;16(3):143-55.
35. Skowron K, Bauza-Kaszewska J, Kraszewska Z, Wiktorczyk-Kapischke N, Grudlewska-Buda K, Kwiecinska-Pirog J, et al. Human Skin Microbiome: Impact of Intrinsic and Extrinsic Factors on Skin Microbiota. Microorganisms. 2021;9(3).
36. Selway CA, Eisenhofer R, Weyrich LS. Microbiome applications for pathology: challenges of low microbial biomass samples during diagnostic testing. J Pathol Clin Res. 2020;6(2):97-106.
37. Mariani J, Favero C, Spinazze A, Cavallo DM, Carugno M, Motta V, et al. Short-term particulate matter exposure influences nasal microbiota in a population of healthy subjects. Environ Res. 2018;162:119-26.
38. Mills JG, Brookes JD, Gellie NJC, Liddicoat C, Lowe AJ, Sydnor HR, et al. Relating Urban Biodiversity to Human Health With the 'Holobiont' Concept. Front Microbiol. 2019;10:550.
39. Hanski I, von Hertzen L, Fyhrquist N, Koskinen K, Torppa K, Laatikainen T, et al. Environmental biodiversity, human microbiota, and allergy are interrelated. Proc Natl Acad Sci U S A. 2012;109(21):8334-9.
40. Kim BR, Shin J, Guevarra R, Lee JH, Kim DW, Seol KH, et al. Deciphering Diversity Indices for a Better Understanding of Microbial Communities. J Microbiol Biotechnol. 2017;27(12):2089-93.
41. Zheng P, Zhang B, Zhang K, Lv X, Wang Q, Bai X. The Impact of Air Pollution on Intestinal Microbiome of Asthmatic Children: A Panel Study. Biomed Res Int. 2020;2020:5753427.
42. Fu P, Bai L, Cai Z, Li R, Yung KKL. Fine particulate matter aggravates intestinal and brain injury and affects bacterial community structure of intestine and feces in Alzheimer's disease transgenic mice. Ecotoxicol Environ Saf. 2020;192:110325.
43. Liu W, Zhou Y, Qin Y, Li Y, Yu L, Li R, et al. Sex-specific effects of PM2.5 maternal exposure on offspring's serum lipoproteins and gut microbiota. Sci Total Environ. 2020;739:139982.
44. Liu Y, Wang T, Si B, Du H, Liu Y, Waqas A, et al. Intratracheally instillated diesel PM2.5 significantly altered the structure and composition of indigenous murine gut microbiota. Ecotoxicol Environ Saf. 2021;210:111903.
45. Ran Z, An Y, Zhou J, Yang J, Zhang Y, Yang J, et al. Subchronic exposure to concentrated ambient PM2.5 perturbs gut and lung microbiota as well as metabolic profiles in mice. Environ Pollut. 2021;272:115987.
46. Wang W, Zhou J, Chen M, Huang X, Xie X, Li W, et al. Exposure to concentrated ambient PM2.5 alters the composition of gut microbiota in a murine model. Part Fibre Toxicol. 2018;15(1):17.
47. Xu Y, Li Z, Liu Y, Pan B, Peng R, Shao W, et al. Differential Roles of Water-Insoluble and Water-Soluble Fractions of Diesel Exhaust Particles in the Development of Adverse Health Effects Due to Chronic Instillation of Diesel Exhaust Particles. Chem Res Toxicol. 2021;34(12):2450-9.
48. Clavel T, Lepage P, Charrier C. The Family Coriobacteriaceae. In: Rosenberg E, DeLong EF, Lory S, Stackebrandt E, Thompson F, editors. The Prokaryotes: Actinobacteria. Berlin, Heidelberg: Springer Berlin Heidelberg; 2014. p. 201-38.

49. Martinez I, Perdicaro DJ, Brown AW, Hammons S, Carden TJ, Carr TP, et al. Diet-induced alterations of host cholesterol metabolism are likely to affect the gut microbiota composition in hamsters. Appl Environ Microbiol. 2013;79(2):516-24.
50. Gomez-Arango LF, Barrett HL, McIntyre HD, Callaway LK, Morrison M, Dekker Nitert M, et al. Connections Between the Gut Microbiome and Metabolic Hormones in Early Pregnancy in Overweight and Obese Women. Diabetes. 2016;65(8):2214-23.
51. Ribiere C, Peyret P, Parisot N, Darcha C, Dechelotte PJ, Barnich N, et al. Oral exposure to environmental pollutant benzo[a]pyrene impacts the intestinal epithelium and induces gut microbial shifts in murine model. Sci Rep. 2016;6:31027.
52. Carr TP, Weller CL, Schlegel VL, Cuppett SL, Guderian DM, Jr., Johnson KR. Grain sorghum lipid extract reduces cholesterol absorption and plasma non-HDL cholesterol concentration in hamsters. J Nutr. 2005;135(9):2236-40.
53. Waters JL, Ley RE. The human gut bacteria Christensenellaceae are widespread, heritable, and associated with health. BMC Biol. 2019;17(1):83.
54. Aleman JO, Bokulich NA, Swann JR, Walker JM, De Rosa JC, Battaglia T, et al. Fecal microbiota and bile acid interactions with systemic and adipose tissue metabolism in diet-induced weight loss of obese postmenopausal women. J Transl Med. 2018;16(1):244.
55. Fu J, Bonder MJ, Cenit MC, Tigchelaar EF, Maatman A, Dekens JA, et al. The Gut Microbiome Contributes to a Substantial Proportion of the Variation in Blood Lipids. Circ Res. 2015;117(9):817-24.
56. Le Roy CI, Beaumont M, Jackson MA, Steves CJ, Spector TD, Bell JT. Heritable components of the human fecal microbiome are associated with visceral fat. Gut Microbes. 2018;9(1):61-7.
57. Lim MY, You HJ, Yoon HS, Kwon B, Lee JY, Lee S, et al. The effect of heritability and host genetics on the gut microbiota and metabolic syndrome. Gut. 2017;66(6):1031-8.
58. Mukherjee A, Lordan C, Ross RP, Cotter PD. Gut microbes from the phylogenetically diverse genus Eubacterium and their various contributions to gut health. Gut Microbes. 2020;12(1):1802866.
59. Wang N, Ma Y, Liu Z, Liu L, Yang K, Wei Y, et al. Hydroxytyrosol prevents PM2.5-induced adiposity and insulin resistance by restraining oxidative stress related NF-kappaB pathway and modulation of gut microbiota in a murine model. Free Radic Biol Med. 2019;141:393-407.
60. Woodby B, Schiavone ML, Pambianchi E, Mastaloudis A, S NH, S MW, et al. Particulate Matter Decreases Intestinal Barrier-Associated Proteins Levels in 3D Human Intestinal Model. Int J Environ Res Public Health. 2020;17(9).
61. Mutlu EA, Engen PA, Soberanes S, Urich D, Forsyth CB, Nigdelioglu R, et al. Particulate matter air pollution causes oxidant-mediated increase in gut permeability in mice. Part Fibre Toxicol. 2011;8:19.
62. Frosali S, Pagliari D, Gambassi G, Landolfi R, Pandolfi F, Cianci R. How the Intricate Interaction among Toll-Like Receptors, Microbiota, and Intestinal Immunity Can Influence Gastrointestinal Pathology. J Immunol Res. 2015;2015:489821.
63. Tilg H, Zmora N, Adolph TE, Elinav E. The intestinal microbiota fuelling metabolic inflammation. Nat Rev Immunol. 2020;20(1):40-54.
64. Saenen ND, Bove H, Steuwe C, Roeffaers MBJ, Provost EB, Lefebvre W, et al. Children's Urinary Environmental Carbon Load. A Novel Marker Reflecting Residential Ambient Air Pollution Exposure? Am J Respir Crit Care Med. 2017;196(7):873-81.
65. He QC, Tavakkol A, Wietecha K, Begum-Gafur R, Ansari SA, Polefka T. Effects of environmentally realistic levels of ozone on stratum corneum function. Int J Cosmet Sci. 2006;28(5):349-57.
66. Cryan JF, O'Riordan KJ, Sandhu K, Peterson V, Dinan TG. The gut microbiome in neurological disorders. Lancet Neurol. 2020;19(2):179-94.
67. Silva YP, Bernardi A, Frozza RL. The Role of Short-Chain Fatty Acids From Gut Microbiota in Gut-Brain Communication. Front Endocrinol (Lausanne). 2020;11:25.
68. Janssen BG, Madhloum N, Gyselaers W, Bijnens E, Clemente DB, Cox B, et al. Cohort Profile: The ENVIRonmental influence ON early AGEing (ENVIRONAGE): a birth cohort study. International Journal of Epidemiology. 2017;46(5):1386-7m.

69. Lefebvre W, Degrawe B, Beckx C, Vanhulsel M, Kochan B, Bellemans T, et al. Presentation and evaluation of an integrated model chain to respond to traffic- and health-related policy questions. Environmental Modelling & Software. 2013;40:160-70.
70. QIAGEN. DNeasy PowerSoil Pro kit handbook 2021 [cited 2022 March 9]. Available from: https://www.qiagen.com/us/resources/resourcedetail?id=9bb59b74-e493-4aeb-b6c1-f660852e8d97&lang=en.
71. QIAGEN. QIAamp DNA Microbiome Handbook 2014 [cited 2022 March 9]. Available from: https://www.qiagen.com/us/resources/resourcedetail?id=c403392b-0706-45ac-aa2e-4a75acd21006&lang=en.

SUPPLEMENTARY SECTION

Modeled air pollution exposure – The residential BC exposure levels were estimated based on a technique described in the articles Cohort profile: The ENVIRonmental influence ON early AGEing by Janssen et al. (68) and Presentation and evaluation of an integrated model chain to respond to traffic- and health-related policy questions by Lefebvre et al. (69). Here, BC exposure levels were interpolated for the residential addresses using the RIO interpolation method, considering CORINE land-cover datasets and pollution data from monitoring stations combined in a dispersion model. The first elements of this dispersion model are Forecasting Evolutionary Activity-Travel of Households and their Environmental RepercussionS (FEATHERS) and Transcad. The FEATHERS model predicts what activities are conducted by individuals in Flanders (Belgium), how long they last, where and when they take place, and how individuals travel to their activity resulting in origin-destination matrixes. These matrixes were then assigned to a road network by applying the Transcad model resulting in the average number of vehicles per road segment. Next, MIMOSA4 was used to estimate hourly traffic emissions of BC based on the previous models. The resulting emission data was then used in an Immission Frequency Distribution model and combined with the RIO model. The latter was used to estimate hourly BC concentrations based on CORINE land-cover data and air pollution data collected in fixed air pollution monitoring stations (n=14 for BC in Flanders, Belgium).

DNeasy PowerSoil Pro kit protocol – The following steps should be performed according to the manufacturer's guidelines (70): **1)** Spin the PowerBead Pro Tubes to ensure that the beads have settled at the bottom. Add up to 250 mg of sample and 800 µl of Solution CD1. Vortex briefly to mix. **2)** Secure the PowerBead Pro Tube horizontally on a Vortex Adapter and vortex at maximum speed for 10 min. **3)** Centrifuge the PowerBead Pro Tube at 15,000 x g for 1 min. **4)** Transfer the supernatant to a 2 ml Microcentrifuge Tube (Expect 500–600 µl). **5)** Add 200 µl of Solution CD2 and vortex for 5 s. **6)** Centrifuge at 15,000 x g for 1 min. Avoiding the pellet, transfer up to 700 µl of supernatant to a clean 2 ml Microcentrifuge Tube (Expect 500–600 µl). **7)** Add 600 µl of Solution CD3 and vortex for 5 s. **8)** Load 650 µl of lysate to an MB Spin Column. Centrifuge at 15,000 x g for 1 min. **9)** Discard the flow-through and repeat step 8 to ensure that all of the lysate has passed through the MB Spin Column. **10)** Carefully place the MB Spin Column into a clean 2 ml Collection Tube. **11)** Add 500 µl of Solution EA to the MB Spin Column. Centrifuge at 15,000 x g for 1 min. **12)** Discard the flow-through and place the MB Spin Column back into the same 2 ml Collection Tube. **13)** Add 500 µl of Solution C5 to the MB Spin Column. Centrifuge at 15,000 x g for 1 min. **14)** Discard the flow-through and place the MB Spin Column into a new 2 ml Collection Tube. **15)** Centrifuge at up to 16,000 x g for 2 min. Carefully place the MB Spin Column into a new 1.5 ml Elution Tube. **16)** Add 50–100 µl of Solution C6 to the center of the white filter membrane. **17)** Centrifuge at 15,000 x g for 1 min to elute the DNA.

QIAamp DNA Microbiome kit protocol – The following steps should be performed according to the manufacturer's guidelines (71): **1)** Add 500 µl Buffer AHL to 1 ml of sample in a 2 ml tube and incubate for 30 min at room temperature with end-over-end rotation. **2)** Centrifuge the tube at 10,000 x g for 10 min and carefully remove the supernatant without disturbing the pellet. **3)** Add 190 µl Buffer RDD and 2.5 µl Benzonase. Mix well and incubate at 37°C for 30 min at 600 rpm in a heating block or water bath. **4)** Add

20 µl of Proteinase K and incubate at 56°C for 30 min at 600 rpm in a heating block or water bath. **5)** Briefly spin the tube at a slow speed to remove condensation. Add 200 µl Buffer ATL (containing Reagent DX), mix well, and transfer into a Pathogen Lysis Tube L. **6)** Lyse bacterial cells with Pathogen Lysis Tube L. Place the Pathogen Lysis Tube L in a TissueLyser LT for 10 min at 50 Hz. **7)** Centrifuge the Pathogen Lysis Tube L at 10,000 x g for 1 min to reduce the amount of foam after lysis. Mix carefully and transfer the supernatant to a fresh microcentrifuge tube. **8)** Add 40 µl of Proteinase K, mix by vortexing, and incubate at 56°C for 30 min at 600 rpm in a heating block or water bath. **9)** Add 200 µl Buffer APL2. Mix by pulse vortexing for 30 s. **10)** Incubate at 70°C for 10 min and briefly spin the tube. **11)** Add 200 µl of ethanol to the lysate. Mix thoroughly by pulse vortexing for 15–30 s. **12)** Carefully apply up to 700 µl of the mixture from step 11 to the QIAamp UCP Mini Column without wetting the rim. Centrifuge at 6,000 x g for 1 min. **13)** Discard the flow-through. Put the column back into the collection tube to repeat step 12 with any remaining mixture from step 11. **14)** Transfer the QIAamp UCP Mini Column to a fresh collection tube. Carefully open the cap and add 500 µl Buffer AW1 without wetting the rim. Close the cap and centrifuge at 6,000 x g for 1 min. Place the QIAamp UCP Mini Column into a fresh 2 ml collection tube and discard the filtrate. **15)** Carefully open the QIAamp UCP Mini Column and add 500 µl Buffer AW2 without wetting the rim. Centrifuge at full speed (20,000 x g) for 3 min. **16)** Place the QIAamp UCP Mini Column into a fresh 2 ml collection tube. Discard the filtrate. Centrifuge at full speed (20,000 x g) for 1 min. **17)** Place the QIAamp UCP Mini Column into a fresh 1.5 ml tube and apply 50 µl Buffer AVE directly onto the center of the membrane. Close the lid and incubate at room temperature for 5 min. **18)** Centrifuge at 6,000 x g for 1 min to elute the DNA.

Supplementary figures and tables – The supplementary figures and tables are shown below.

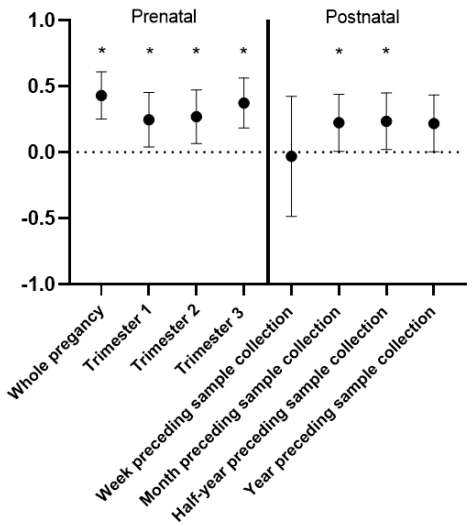

Fig. S1 – Correlation of measured prenatal BC and black carbon in cord blood and postnatal measured BC exposure and BC in urine. BC: black carbon

* Significant p-values ($p<0.05$)

Table S1– Percentual changes in diversity and richness indices after quadrupling of green space exposure

	Estimate	Lower 95% CI	Upper 95% CI	p-value
Low green 50m				
Shannon	16.51	-0.99	37.10	0.066+
Simpson	2.66	-0.50	5.92	0.100
Chao	41.99	-10.31	124.81	0.135
Low green 100m				
Shannon	15.90	-2.89	38.31	0.102
Simpson	2.43	-0.87	5.83	0.151
Chao	36.42	-18.25	127.65	0.235
Low green 300m				
Shannon	17.01	-6.12	45.82	0.162
Simpson	2.87	-1.34	7.27	0.184
Chao	44.61	-26.51	184.59	0.286
Low green 500m				
Shannon	7.29	-15.75	36.61	0.568
Simpson	1.56	-3.14	6.49	0.522
Chao	23.70	-39.01	150.91	0.556
Low green 1000m				
Shannon	5.58	-19.10	37.79	0.689
Simpson	1.11	-4.03	6.53	0.678
Chao	7.44	-50.25	132.01	0.855
Low green 2000m				
Shannon	-0.46	-27.11	35.94	0.977
Simpson	0.37	-5.57	6.68	0.906
Chao	-9.80	-63.12	120.62	0.821
Low green 3000m				
Shannon	-6.43	-32.42	29.54	0.689
Simpson	0.45	-6.69	6.21	0.893
Chao	-23.29	-70.18	97.34	0.582
High green 50m				
Shannon	-1.45	-14.14	13.11	0.835
Simpson	-1.37	-4.02	1.36	0.323
Chao	23.54	-19.18	88.84	0.329
High green 100m				
Shannon	-4.11	-17.08	10.88	0.571
Simpson	-1.84	-4.71	1.12	0.220
Chao	16.83	-24.92	81.78	0.491
High green 300m				
Shannon	-6.23	-18.84	8.34	0.383

Simpson	-1.55	-4.36	1.35	0.292
Chao	-3.20	-37.49	49.89	0.884
High green 500m				
Shannon	-4.60	-16.95	9.60	0.506
Simpson	-1.02	-3.82	1.86	0.483
Chao	0.35	-34.11	52.84	0.987
High green 1000m				
Shannon	-4.57	-16.59	9.18	0.496
Simpson	-1.29	-3.91	1.39	0.342
Chao	4.18	-30.26	55.63	0.842
High green 2000m				
Shannon	-4.76	-16.47	8.59	0.466
Simpson	-1.43	-4.03	1.24	0.291
Chao	12.60	-23.52	65.79	0.548
High green 3000m				
Shannon	-2.50	-14.87	11.67	0.715
Simpson	-0.95	-3.66	1.83	0.498
Chao	23.33	-70.18	97.34	0.302
Total green 50m				
Shannon	7.68	-4.62	21.57	0.232
Simpson	0.468	-1.88	2.87	0.698
Chao	47.14	2.38	111.47	0.037*
Total green 100m				
Shannon	6.75	-7.59	23.31	0.375
Simpson	-0.05	-2.88	2.85	0.971
Chao	49.41	-3.78	132.01	0.074^{+}
Total green 300m				
Shannon	0.12	-13.50	15.89	0.987
Simpson	-0.31	-3.19	2.65	0.834
Chao	16.05	-25.34	80.40	0.508
Total green 500m				
Shannon	-2.01	-15.16	13.17	0.782
Simpson	-0.45	-3.33	2.52	0.766
Chao	9.43	-28.14	66.65	0.675
Total green 1000m				
Shannon	-2.77	-14.71	10.84	0.674
Simpson	-0.85	-3.46	1.82	0.527
Chao	6.24	-27.74	56.18	0.758
Total green 2000m				

Shannon	-3.83	-14.36	8.00	0.509
Simpson	-1.08	-3.38	1.28	0.368
Chao	8.91	-22.91	53.87	0.628
Total green 3000m				
Shannon	-2.89	-13.89	9.51	0.632
Simpson	-0.82	-3.18	1.60	0.503
Chao	14.38	-19.80	63.12	0.458

Robust linear regression analyses between green spaces and Shannon diversity, Simpson diversity, or Chao richness are shown after adjustment for parity, ponderal index, age, gender, diploma of the mother and batch. Results are expressed as a percentual change for each quadrupling in green space. CI: confidence interval; BC: black carbon

* Significant p-values ($p<0.05$)

$^{+}$ p-values indicating a trend ($p<0.10$)